

^{129}Xe NMR shielding and self-diffusion in the mixture of two thermotropic nematogens with opposite diamagnetic anisotropy

Jyrki Ruohonen and Jukka Jokisaari*

NMR Research Group, Department of Physical Sciences, P.O. Box 3000, FIN-90014 University of Oulu, Finland. E-mail: Jukka.Jokisaari@oulu.fi

Received 27th March 2001, Accepted 5th June 2001

First published as an Advance Article on the web 4th July 2001

The nuclear shielding and self-diffusion coefficient of xenon-129 dissolved in the so-called critical mixture of two nematic liquid crystals with opposite diamagnetic anisotropy were determined as a function of temperature applying ^{129}Xe NMR spectroscopy. In the critical mixture, the liquid crystal director rotates 90° from the parallel direction to the perpendicular one with respect to the external magnetic field when approaching the critical point from high temperature side. The director reorientation offers a straightforward means to determine the self-diffusion coefficients of xenon, D_{\parallel} and D_{\perp} , in the parallel and perpendicular directions, respectively, relative to the liquid crystal director simply by applying pulsed Z-gradient only. The self-diffusion tensor was found to be slightly anisotropic, the ratio D_{\perp}/D_{\parallel} being *ca.* 0.78, over the whole temperature range investigated. The fit of a theoretical model function to the experimental shielding data gives the ^{129}Xe shielding constant, σ_0 , and the anisotropy of the shielding tensor, $\Delta\sigma_0$, as well as the density change at the isotropic–nematic phase transition. Furthermore, temperature dependence of shielding and shielding anisotropy can be determined with the help of the adjusted parameters.

Introduction

^{129}Xe NMR shielding of xenon dissolved in liquid crystals (LCs) gives versatile information on the LC behavior. In particular, when the shielding is measured at variable temperatures various properties may be determined; such as the sign of the anisotropy of the diamagnetic susceptibility tensor, $\Delta\chi_d$, of the LC, phase transitions and phase diagrams, and orientational order parameters.^{1–4} Recently, a theory based on a statistical mechanical approach was presented. According to this model, in the pairwise additivity approximation of shielding perturbations the isotropic and anisotropic contributions of the experimentally observable noble gas shielding are dependent upon the LC density and the latter depends furthermore on the second rank LC orientational order parameter.⁵

When a liquid crystalline sample is placed in an external magnetic field with flux density B_0 , the sample becomes magnetized and the magnetic energy density is⁶

$$\rho_B = -\frac{B_0^2}{2\mu_0} [\chi_d + \frac{2}{3}\Delta\chi_d P_2(\cos \theta)], \quad (1)$$

where μ_0 is permeability of a vacuum, and χ_d and $\Delta\chi_d$ are the isotropic average and anisotropy of the diamagnetic volume susceptibility tensor χ_d , respectively. $P_2(\cos \theta) = \frac{1}{2}(3 \cos^2 \theta - 1)$ is the second order Legendre polynomial with θ being the angle between the LC director \mathbf{n} and the external magnetic field \mathbf{B}_0 . Keeping in mind that χ_d is negative whereas $\Delta\chi_d$ may be either negative or positive and considering the minimum energy density condition, one may derive the following conclusions: (a) the orientation of the LC director, \mathbf{n} , with respect to the external magnetic field is determined by the sign of $\Delta\chi_d$, and (b) if the sign is positive, \mathbf{n} orients parallel with the external magnetic field, \mathbf{B}_0 , while if the sign is negative, \mathbf{n} orients perpendicular to \mathbf{B}_0 .

When two LCs are mixed, the anisotropy of the diamagnetic susceptibility is a weighted average of the $\Delta\chi_d$'s of

the components:^{7,8}

$$\Delta\chi_d = v\Delta\chi_{dI} + (1 - v)\Delta\chi_{dII}, \quad (2)$$

where $\Delta\chi_{dI}$ and $\Delta\chi_{dII}$ are the anisotropy of the diamagnetic susceptibility of components I and II, respectively, and v is the volume fraction of the component I. The volume diamagnetic anisotropy of each component may be represented by⁷

$$\Delta\chi_{di} = \frac{\rho_i(T)}{M_i} \Delta\chi_i^m S(T) \quad (3)$$

where $i = \text{I or II}$, $\rho(T)$ is the density, M is the molar mass, $\Delta\chi^m$ is the anisotropy of the molecular susceptibility tensor (essentially independent of temperature), and $S(T)$ is the second rank orientational order parameter.

From eqns. (1)–(3), one may conclude that when mixing two thermotropic nematic liquid crystals, one with a negative and the other one with a positive diamagnetic anisotropy, in an appropriate volume ratio it is possible to reach by the changing sample temperature the so-called critical point at which the total $\Delta\chi_d$ vanishes. On the high temperature side of the critical point $\Delta\chi_d > 0$, and thus \mathbf{n} is parallel with \mathbf{B}_0 , whereas on the low temperature side $\Delta\chi_d < 0$ and \mathbf{n} is perpendicular to \mathbf{B}_0 . At the exact critical condition the LC sample consists of an isotropic orientational distribution of molecules. However, it is extremely difficult to reach and maintain the exact critical condition because it requires accurate temperature regulation and a vanishing temperature gradient, and therefore only a distribution of domains of variable size and orientation may be detected, and the NMR spectrum of LC molecules or solute molecules resembles a powder pattern.⁹

In the present study, we have measured the ^{129}Xe shielding with respect to an external low-pressure gas reference as a function of temperature for xenon in the mixture of two nematic LCs: ZLI1167 with negative $\Delta\chi_d$ and EBBA- d_2 with positive $\Delta\chi_d$, which when mixed properly generate the critical condition described above. The recently developed theoretical model was applied to interpret the data. Furthermore, we utilized a LC director rotation of 90° at the critical point for the

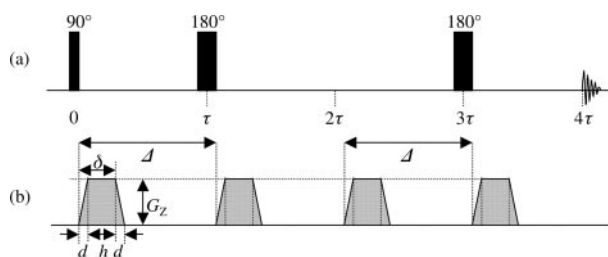


Fig. 1 Convection compensating DSE pulse sequence¹⁰ used for self-diffusion measurements: (a) radiofrequency and (b) gradient pulses. Diffusion is encoded by varying the gradient strength G_z , while the total measurement time (4τ) was kept constant, i.e. signal attenuation due to transverse relaxation is constant. Phase cycling of radiofrequency pulses and receiver are as in ref. 10.

measurement of the ^{129}Xe self-diffusion coefficients, D_{\parallel} and D_{\perp} , at the two orientations of the director.

Experimental

The ^{129}Xe shielding and self-diffusion experiments were performed for ^{129}Xe enriched (70%) xenon gas dissolved in the mixture of Merck ZLI1167 (77 wt.%) and EBBA- d_2 (4-ethoxybenzylidene-2,6-dideutero-4'-*n*-butylaniline; 23 wt.%). ZLI1167 is composed of three 4-*n*-alkyl-*trans,trans*-bicyclohexyl-4'-carbonitriles and possesses negative anisotropy of diamagnetic susceptibility. EBBA- d_2 has a positive diamagnetic anisotropy. The sample was placed in a 5 mm glass tube and carefully degassed prior to xenon gas transfer (equilibrium pressure *ca.* 1.8 atm) and flame sealing. All the experiments were performed on a Bruker Avance DRX500 spectrometer equipped with 5 mm Bruker inverse broadband probe with integrated Z-gradient coils (gradient in the direction of the external magnetic field; maximum gradient strength 0.566 T m^{-1}). For ^{129}Xe , the DRX500 operates at 138.8 MHz. The temperature was calibrated with a sample of ethylene glycol (80%) in DMSO.

The self-diffusion measurements were carried out by the convection compensating double spin echo (DSE) pulse sequence with ramped Z-gradient pulses as described in ref. 10 (see Fig. 1). The diffusion data were acquired with eight different values of the gradient strength so that the first gradient value is zero, accumulating 16 scans and keeping the total measurement time 4τ constant. Furthermore, the ratio of the minimum to maximum signal amplitude was about 0.1. The parameters used, which are shown in Fig. 1, were: $G_z = 0$ – 0.566 T m^{-1} , $\Delta = 66$ – 146 ms , $\delta = 5 \text{ ms}$ and $d = 0.8 \text{ ms}$. The 90° pulse repetition time ($-5 \times T_1$) was chosen according to the measured longitudinal relaxation times T_1 of ^{129}Xe in both phases. In the isotropic phase the measured T_1 was *ca.* 40 s whereas in the nematic phase it shortened from about 30 s to 20 s with decreasing temperature. The measurements were started by warming the sample to 351.9 K (isotropic phase) and then cooling in 2.3 K temperature intervals over the isotropic–nematic phase transition and critical point to 300.8 K. The ^{129}Xe shielding was referenced to the low-pressure pure gas signal at 299.7 K.

Results and discussion

A. ^{129}Xe shielding

The average of the shielding tensor element in the direction of the external magnetic field (Z) can be represented in the form⁵

$$\langle \sigma_{zz} \rangle = \rho(T) \{ \sigma_0 [1 - \varepsilon(T - T_0)] + \frac{2}{3} \Delta \sigma_0 [1 - \Delta \varepsilon(T - T_0)] P_2(\cos \theta) S(T) \}, \quad (4)$$

where σ_0 and $\Delta \sigma_0$ are the shielding constant and shielding anisotropy, respectively, at the reference temperature T_0 . The coefficients ε and $\Delta \varepsilon$ describe the temperature dependence (assumed to be linear) of shielding and shielding anisotropy, respectively. The other parameters have the meaning as explained in the Introduction. The temperature dependence of the density of the present LC is not known. It is, however, a good approximation to assume a linear dependence:¹¹ $\rho(T) = \rho_0 [1 - \alpha(T - T_0)]$, where ρ_0 is the density at the reference temperature and α is the isobaric thermal expansion coefficient. In the various phases (isotropic and nematic ones in the present case) α is not necessarily the same, and, moreover, the density is discontinuous at the isotropic–nematic phase transition. Thus, in the nematic phase the density is described by the function: $\rho(T) = \rho_0 \{ [1 - \alpha(T - T_0)] + \Delta \rho / \rho_0 \}$, where $\Delta \rho$ is the density jump in the isotropic–nematic phase transition. The temperature dependence of the second rank orientational order parameter was described by the Haller function $S(T) = (1 - yT/T_{\text{NI}})^z$, where T_{NI} is the isotropic–nematic phase transition temperature (chosen to be the reference temperature T_0), and y and z are adjustable parameters.¹²

Fig. 2 shows the measured ^{129}Xe NMR spectrum of xenon gas dissolved in the critical mixture of Merck ZLI1167 and EBBA- d_2 at different temperatures. Because the ^{129}Xe shielding was measured relative to an external low-pressure gas sample, a bulk susceptibility correction, σ_b , has to be applied to get the pure medium effect on the shielding. For a long cylindrical sample with its axis parallel with the external magnetic field, the correction may be calculated from¹³

$$\sigma_b = -\frac{1}{3} [\chi_d + \frac{2}{3} \Delta \chi_d S(T)] \frac{\rho(T)}{M}, \quad (5)$$

where both χ_d and $\Delta \chi_d$ are given in $\text{m}^3 \text{ mol}^{-1}$. Neither χ_d nor $\Delta \chi_d$ is known for the present ZLI1167/EBBA- d_2 mixture. Therefore, χ_d/M was chosen to be $-8.87 \times 10^{-9} \text{ m}^3 \text{ kg}^{-1}$ ($\chi_d = -2.56 \times 10^{-9} \text{ m}^3 \text{ mol}^{-1}$ when a molar mass of $0.289 \text{ kg mol}^{-1}$ is used), which is the value for one of the three components of ZLI1167.¹⁴ As we are dealing with a LC mixture with vanishingly small, though slightly positive or negative, $\Delta \chi_d$, we can omit the latter term in eqn. (5) without introducing any significant error, in particular when keeping in mind the approximate value for χ_d .

The least-squares fit to eqn. (4) was carried out in two stages: first, the isotropic–nematic phase transition temperature, $T_{\text{NI}} = T_0$, was fixed to 343.8 K and the parameters σ_0 , ε , ρ_0 and α were adjusted for the isotropic phase in which the second part of eqn. (4) vanishes (because $S = 0$), and secondly, σ_0 , ε and ρ_0 were kept fixed to the values obtained in the isotropic phase whereas $\Delta \sigma_0$, α , $\Delta \varepsilon$, $\Delta \rho / \rho_0$ and z were adjusted. The other parameter, y , in the Haller function was chosen to be 0.9988, which was the value of y for pure EBBA- d_2 .⁵ The experimental shielding values and the results of the least-squares fits are shown in Fig. 3. The values of the adjusted parameters are collected in Table 1. Fig. 4 in turn shows the orientational order parameter S as a function of temperature.

The fit results in a density ρ_0 of $0.975 \pm 0.001 \text{ g cm}^{-3}$ and a relative density jump $\Delta \rho / \rho_0$ of $(0.55 \pm 0.02)\%$ at the isotropic–nematic phase transition temperature $T_{\text{NI}} = T_0 = 343.8 \text{ K}$. The corresponding data are not known for the present mixture or ZLI1167. For pure EBBA, they are 0.989 g cm^{-3} and 0.26% , respectively, which are very similar to what is obtained here.¹⁵ One should, however, point out that the T_{NI} of pure EBBA is *ca.* 352.5 K and that the present mixture consists of only *ca.* 23 wt.% EBBA- d_2 . The calculated ^{129}Xe shielding jump due to the density jump at the isotropic–nematic phase transition is *ca.* -1.1 ppm (see Fig. 3), which is in good agreement with the earlier estimated value of -1 ppm .¹ The thermal expansion coefficients α derived for the isotropic and nematic phases

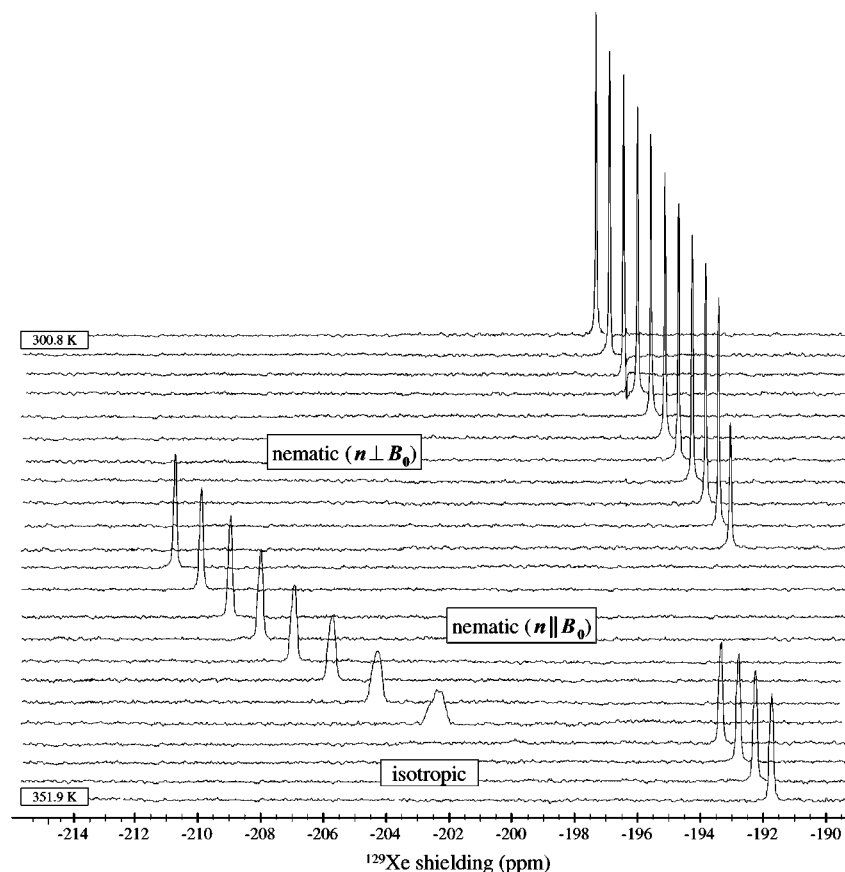


Fig. 2 ^{129}Xe NMR spectrum of xenon gas dissolved in the critical mixture of Merck ZLI1167 and EBBA- d_2 as a function of temperature with a step of 2.3 K. The shielding values are given with respect to the shielding of external low-pressure xenon gas and the shielding scale is defined as positive to low frequency. Each spectrum was from a DSE experiment without field gradient pulses (see Fig. 1). In the isotropic–nematic phase transition the ^{129}Xe shielding abruptly decreases *ca.* 9 ppm. Conversely, due to the 90° rotation of the LC director \mathbf{n} at the critical point the ^{129}Xe shielding abruptly increases about 18 ppm. Line broadening near the isotropic–nematic phase transition is caused by instabilities, *e.g.* temperature gradients and fluctuations, in the sample tube.

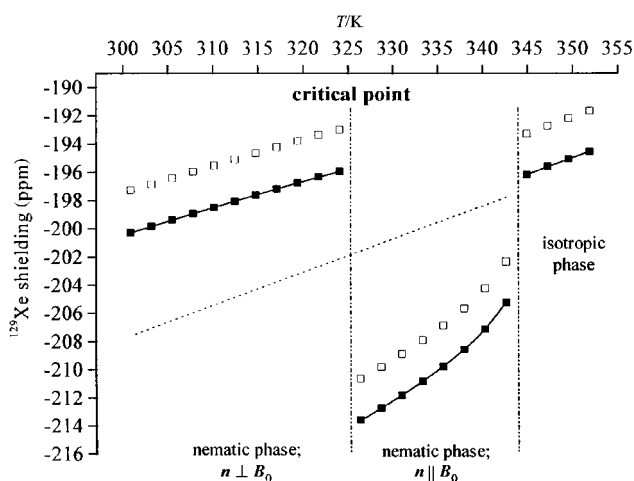


Fig. 3 ^{129}Xe shielding (referenced to an external low-pressure xenon gas sample) as a function of temperature T for xenon in the ZLI1167/EBBA- d_2 LC mixture. (□) Correspond to shielding without bulk susceptibility correction; (■) shielding corrected for bulk susceptibility. The solid lines represent least-squares fits to eqn. (4). The abrupt change at 343.8 K indicates the isotropic–nematic phase transition. The other abrupt change at about 325 K is due to the rotation of the LC director from the parallel (high temperature) to the perpendicular (low temperature) direction with respect to the external magnetic field (so-called critical point). The calculated isotropic average of the ^{129}Xe shielding tensor, *i.e.* the isotropic part of eqn. (4), in the nematic phase is indicated by the dotted line. The density jump causes the jump of the isotropic average of the ^{129}Xe shielding tensor at the isotropic–nematic phase transition. The dashed vertical lines denote the isotropic–nematic phase transition and the critical point.

are $8.3 \pm 0.3 \times 10^{-4} \text{ K}^{-1}$ and $8.2 \pm 0.1 \times 10^{-4} \text{ K}^{-1}$, respectively, which are very typical for thermotropic nematogens.¹¹ For example, for pure EBBA the respective values are $8.09 \times 10^{-4} \text{ K}^{-1}$ and $9.92 \times 10^{-4} \text{ K}^{-1}$.¹⁵ The temperature dependence of the ^{129}Xe shielding and shielding anisotropy (*i.e.* the coefficients ϵ and $\Delta\epsilon$) are qualitatively similar to what was observed for pure EBBA- d_2 .⁵ However, in particular, $\Delta\epsilon$ is about one order of magnitude smaller than in EBBA- d_2 but it is still negative, which indicates that in the present LC mixture the average anisotropy of the local shielding tensor (*i.e.* the anisotropic part of eqn. (4) without the orientational

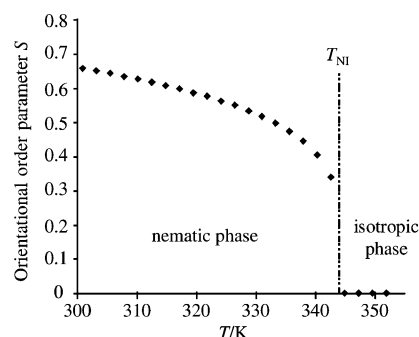


Fig. 4 The second rank orientational order parameter (with respect to the LC director), S , of the ZLI1167/EBBA- d_2 mixture as a function of temperature T . The isotropic–nematic phase transition temperature $T_{\text{NI}} = 343.8 \text{ K}$ is indicated by the vertical dashed line. Due to the random orientations of the LC molecules, the orientational order parameter S is zero in the isotropic phase.

Table 1 Values of the parameters derived from the least-squares fits of eqn. (4) to the experimental ^{129}Xe shielding data

Parameter	Isotropic phase ^a	Nematic phase ^c
$T_0 = T_{\text{NI}}/\text{K}$	343.8 ^b	343.8 ^b
$\rho_0/\text{g cm}^{-3}$	0.975 ± 0.001	0.975 ^c
$\Delta\rho/\rho_0$ (%)	—	0.55 ± 0.02
$\alpha/10^{-4} \text{ K}^{-1}$	8.3 ± 0.3	8.2 ± 0.1
$\sigma_0/\text{ppm cm}^3 \text{ g}^{-1}$	-201.5 ± 0.1	-201.5^c
$\varepsilon/10^{-4} \text{ K}^{-1}$	3.7 ± 0.3	3.7 ^c
$\Delta\sigma_0/\text{ppm cm}^3 \text{ g}^{-1}$	—	-32.7 ± 0.3
$\Delta\varepsilon/10^{-4} \text{ K}^{-1}$	—	-1.6 ± 1.4
y	—	0.9988 ^d
z	—	0.197 ± 0.003

^a The errors are probable errors of the least-squares fits to eqn. (4). The real errors are obviously larger due to experimental errors of the temperature and the ^{129}Xe shielding. ^b Fixed (see the text). ^c Fixed to the value obtained in the isotropic phase. ^d Chosen on the basis of other works⁵ and kept constant.

order parameter) also decreases with decreasing temperature.⁵ Also, the fitted result for the parameter z of the Haller function, 0.197 ± 0.003 , is close to the previous value of 0.182 for pure EBBA- d_2 . Due to the parameter y (slightly smaller than one, in the present case fixed to 0.9988) in the Haller function the orientational order parameter $S(T = T_{\text{NI}}) = (1 - y)^2$ at the isotropic–nematic phase transition temperature T_{NI} has a non-zero value of 0.266, which is consistent with the Maier–Saupe theory.¹⁶

B. ^{129}Xe self-diffusion

In the present DSE experiment with ramped gradient pulses,¹⁰ the self-diffusion coefficient D was determined from the attenuation of the signal amplitudes,

$$\frac{A(4\tau, G_z)}{A_0(4\tau, 0)} = \exp\left\{-2\gamma^2 G_z^2 D \left[\delta^2 \left(A - \frac{\delta}{3}\right) + \frac{d^3}{30} - \frac{\delta d^2}{6}\right]\right\}, \quad (6)$$

where the notations of Fig. 1 have been used. $A(4\tau, G_z)$ and $A_0(4\tau, 0)$ are the signal amplitudes with and without field gradient pulses, respectively, and γ is the gyromagnetic ratio of the nucleus. Because the diffusion was encoded by varying the strength of the gradient pulses and keeping the total measurement time (4τ) constant, the signal attenuation due to transverse relaxation, $\exp(-4\tau/T_2)$, is constant. The self-diffusion coefficients were calculated by performing a least-squares fit of eqn. (6) to experimental points. The resulting values of the ^{129}Xe self-diffusion coefficient in parallel direction to the external magnetic field B_0 are plotted on a logarithmic scale as a function of reciprocal temperature in Fig. 5. The solid lines in Fig. 5 are the least-squares fits of the Arrhenius equation, $D = D_0 \exp(E_a/RT)$, where E_a is the activation energy, R is the universal gas constant ($8.3145 \text{ J mol}^{-1} \text{ K}^{-1}$) and D_0 is the pre-exponential factor. The isotropic–nematic phase transition temperature and the critical point are defined by the ^{129}Xe shielding data. The results of the Arrhenius fits, the pre-exponential factor D_0 and the activation energy E_a in the isotropic and in the nematic phase at parallel and perpendicular orientations of the LC director n with respect to B_0 , are given in Table 2.

In the isotropic phase, in which random orientations of the LC molecules appear, the measured self-diffusion coefficient of ^{129}Xe , D_{iso} , is independent of the direction of the measurement and it is equal to $\frac{1}{3}$ of the trace of the second rank ^{129}Xe self-diffusion tensor D . The value of the activation energy in the isotropic phase, $E_{\text{iso}} 19.9 \pm 3.7 \text{ kJ mol}^{-1}$, is within the same error limits as for xenon in the isotropic phase of the ferroelectric FELIX-R&D LC [$22.3 \pm 1.6 \text{ kJ mol}^{-1}$].¹⁰ In the phase transition from the isotropic to the nematic phase, in which n orients parallel with B_0 (as concluded above), the

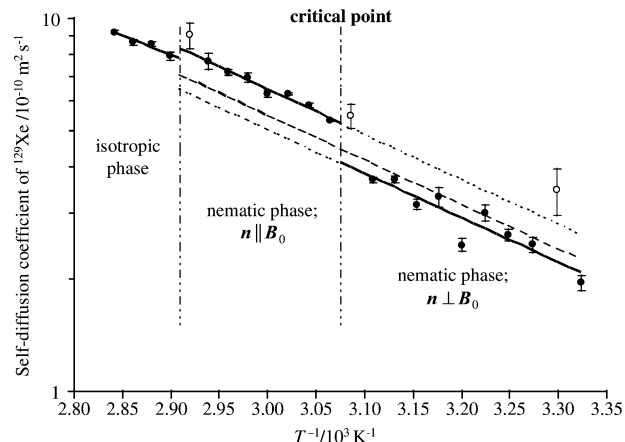


Fig. 5 The ^{129}Xe self-diffusion coefficient in the direction of the external magnetic field B_0 as a function of reciprocal temperature T^{-1} for xenon dissolved in the critical ZLI1167/EBBA- d_2 mixture. The solid lines represent the Arrhenius fits to the experimental points (●) whereas the dotted lines were obtained by extrapolation. Error bars denote the probable errors from the least-square fits of the DSE eqn. (6) to the experimental data. Dashed vertical lines indicate the isotropic–nematic phase transition and critical point according to the ^{129}Xe shielding data. The open circles correspond to the points that were omitted from the fits due to large errors. Near the isotropic–nematic phase transition and the critical point the large errors originate, probably, from instabilities, e.g. temperature gradients and fluctuations in the sample tube. The calculated isotropic average $\langle D \rangle = \frac{1}{3}(D_{\parallel} + 2D_{\perp})$ is indicated by the dashed line.

measured ^{129}Xe self-diffusion coefficient increases and the self-diffusion behavior is clearly discontinuous (Fig. 5). Another discontinuity is detected at the critical point, where n rotates by 90° and the ^{129}Xe self-diffusion coefficient decreases abruptly. Near the isotropic–nematic phase transition and the critical point and at one temperature in the nematic phase the measured ^{129}Xe self-diffusion coefficients deviate very clearly from the Arrhenius fits and, moreover, the error limits are large (Fig. 5). Thus the corresponding points have been omitted from the Arrhenius fits. Close to the isotropic–nematic phase transition and the critical point the orientational order of the liquid crystal is very sensitive to temperature gradients and fluctuations, and evidently such instabilities in the system can induce the scattering of the measured ^{129}Xe self-diffusion coefficients. In the ^{129}Xe spectrum the instabilities cause clear line broadening near the isotropic–nematic phase transition (Fig. 2).

The self-diffusion measurements carried out in the direction parallel with the external magnetic field on both sides of the critical point yield the ^{129}Xe self-diffusion coefficients, D_{\parallel} and D_{\perp} , and the respective activation energies, E_{\parallel} and E_{\perp} , at the two orientations of the director in the nematic phase. The subscripts refer to the orientation of n with respect to B_0 . The obtained activation energies E_{\parallel} and E_{\perp} are equal and only slightly greater than the value of the activation energy in the isotropic phase (Table 2). Also, earlier investigations for the

Table 2 The pre-exponential factor, D_0 , and the activation energy, E_a , derived from the fit of the Arrhenius equation to the experimental ^{129}Xe self-diffusion coefficients determined at variable temperatures

Phase	$D_0/\text{m}^2 \text{ s}^{-1a}$	$E_a/\text{kJ mol}^{-1b}$
Isotropic	8.29×10^{-7}	19.9 ± 3.7
Nematic ($n \parallel B_0$)	2.58×10^{-6}	23.0 ± 1.6
Nematic ($n \perp B_0$)	1.8910^{-6}	22.8 ± 3.7

^a The pre-exponential factor simply reproduces the experimental self-diffusion coefficient over a certain temperature range, i.e. it has no real physical significance, and, therefore, no error is given. ^b The errors are the probable errors of the Arrhenius fits.

spherical TMS molecule in the nematic phase of the MBBA (*p*-methoxybenzylidene-*p*'-*n*-butylaniline) and Merck Phase IV (eutectic mixture of *p*-methoxy-*p*'-*n*-butylazoxybenzenes) LC's have shown that $E_{\parallel} \approx E_{\perp}$.¹⁷ One should keep in mind that the pre-exponential factor D_0 and the activation energy E_a are constants only within a phase.^{10,17} The behavior of D_{\parallel} and D_{\perp} as a function of reciprocal temperature was extrapolated over the whole nematic phase (Fig. 5) and consequently the anisotropy of the ^{129}Xe self-diffusion tensor \mathbf{D} can be defined in the nematic phase. The obtained ratio of the self-diffusion coefficients, D_{\perp}/D_{\parallel} , varies from 0.780 to 0.787 when moving from the isotropic–nematic phase transition temperature to 300.8 K, being 0.783 at the critical point. This is consistent with the previous conclusion that the self-diffusion of small globular objects in the nematic phase is only slightly anisotropic, *i.e.* the ratio D_{\perp}/D_{\parallel} is close to unity.¹⁰ However, in contrast to the nematic phase of the ferroelectric FELIX-R&D LC, where the measured ratio D_{\perp}/D_{\parallel} for xenon was 1.6 ± 0.3 ,¹⁰ it is smaller than unity in the present LC mixture, as observed for TMS in the nematic phase of the MBBA and Merck Phase IV LC's.¹⁷ The observed equal activation energies E_{\parallel} and E_{\perp} demonstrate that the ^{129}Xe self-diffusion anisotropy depends mainly on long-range orientation of the LC molecules in the nematic phase, contrary to the smectic phases where the self-diffusion anisotropy depends primarily on the strongly different activation energies within or perpendicular to the smectic layers.¹⁷

Because of the uniaxial symmetry of the nematic phase the self-diffusion tensor is cylindrically symmetric with respect to \mathbf{B}_0 , and the isotropic average $\langle D \rangle$ can be calculated from $\frac{1}{3}(D_{\parallel} + 2D_{\perp})$. At the isotropic–nematic phase transition point the calculated $\langle D \rangle$ is *ca.* $0.7 \times 10^{-10} \text{ m}^2 \text{ s}^{-1}$ smaller than the extrapolated D_{iso} (Fig. 5). Such a result is in agreement with the theory in which the generalized free volume approach is used to evaluate diffusion coefficient of the small hard-sphere tracer (*i.e.* spherical self-diffusion object) in the nematic phase.¹⁸ In this model the difference between the D_{iso} and the $\langle D \rangle$ originates from the orientation dependent component of the density, the free-volume, which is visualized as a system of rigid tubelike shells, polydisperse in length, dissolved in the rodlike matrix.¹⁸

Conclusions

We have applied ^{129}Xe NMR spectroscopy to study xenon shielding and self-diffusion as a function of temperature in the so-called critical mixture of two nematic liquid crystals with opposite diamagnetic anisotropy. The LC director reorientation at the critical point was utilized for the measurement of the ^{129}Xe self-diffusion coefficients, D_{\parallel} and D_{\perp} , at the two orientations of the director by using the pulsed Z-gradient only. The self-diffusion measurements were performed by using the DSE experiment to avoid convection problems at the elevated temperatures. The shielding data were interpreted

by using a recently developed theoretical model,⁵ which yielded the isotropic ^{129}Xe shielding constant, the anisotropy of the shielding tensor, the thermal expansion coefficients in the isotropic and nematic phases as well as the density change at the isotropic–nematic phase transition. Moreover the parameters, which describe the additional temperature dependence of shielding and shielding anisotropy, are given by the fitting of the results. The self-diffusion experiments reveal the discontinuous self-diffusion behavior of xenon at the isotropic–nematic phase transition and at the critical point. The observed self-diffusion coefficient D_{\parallel} in the parallel direction with the LC director was found to be somewhat larger than the self-diffusion coefficient D_{\perp} in the perpendicular direction to the director, the self-diffusion tensor being consequently slightly anisotropic. The corresponding activation energies E_{\parallel} and E_{\perp} were found to be equal, and, thus, the anisotropy of the self-diffusion tensor is practically independent of temperature. The similar activation energies E_{\parallel} and E_{\perp} indicate that the self-diffusion anisotropy originates mainly from long-range orientation of the LC molecules in the nematic phase. A non-negligible difference was found between the extrapolated D_{iso} and the calculated isotropic average $\langle D \rangle$ which is consistent with the theory¹⁸ presented previously.

Acknowledgements

We thank the Academy of Finland and Neste Oy Foundation for financial support.

References

- 1 J. Jokisaari and P. Diehl, *Liquid Crystals*, 1990, **7**, 739.
- 2 J. Jokisaari, P. Diehl and O. Münster, *Mol. Cryst. Liq. Cryst.*, 1990, **188**, 189.
- 3 J. Lounila, O. Münster, J. Jokisaari and P. Diehl, *J. Chem. Phys.*, 1992, **97**, 8977.
- 4 J. Jokisaari, *Prog. NMR Spectrosc.*, 1994, **26**, 1.
- 5 M. Ylihautila, J. Lounila and J. Jokisaari, *J. Chem. Phys.*, 1999, **110**, 6381.
- 6 P. G. de Gennes and J. Prost, in *The Physics of Liquid Crystals*, 2nd edn., Oxford Science Publications, Oxford, 1993.
- 7 Hp. Schad, G. Baur and G. Meier, *J. Chem. Phys.*, 1979, **71**, 3174.
- 8 P. Diehl and J. Jokisaari, *Chem. Phys. Lett.*, 1982, **87**, 494.
- 9 J. Jokisaari and Y. Hiltunen, *Chem. Phys. Lett.*, 1985, **115**, 441.
- 10 J. Ruohonen, M. Ylihautila and J. Jokisaari, *Mol. Phys.*, 2001, **99**, 711.
- 11 W. Wedler, in *Handbook of Liquid Crystals*, ed. D. Demus, J. Goodby, G. W. Gray, H.-W. Spiess and V. Vill, Wiley-VCH, Weinheim, 1998, vol. 1, pp. 334–350.
- 12 I. Haller, *Prog. Solid State Chem.*, 1975, **10**, 103.
- 13 A. D. Buckingham and E. D. Burnell, *J. Am. Chem. Soc.*, 1967, **89**, 3341.
- 14 J. D. Bunning, D. A. Crellin and T. E. Faber, *Liq. Cryst.*, 1986, **1**, 37.
- 15 B. Bahadur and S. Chandra, *J. Phys. C*, 1976, **9**, 5.
- 16 W. Maier and A. Saupe, *Z. Naturforsch., A: Phys. Sci.*, 1960, **15**, 287.
- 17 G. J. Krüger, *Phys. Rep.*, 1982, **82**, 229.
- 18 D. Sokolowska and J. K. Moscicki, *Phys. Rev. E*, 1996, **54**, 5221.